Postprint
Tree physiology (ISSN 1758-4469), 2020
DOI 10.1093/treephys/tpaa030

Post-fire effects on development of leaves and secondary vascular tissues in *Quercus pubescens*

Authors: Jožica Gričar[1*], Polona Hafner[1], Martina Lavrič[1], Mitja Ferlan[1], Nives Ogrinc[2], Bor Krajnc[2], Klemen Eler[1,3], Dominik Vodnik[3]

[1]Department of Yield and Silviculture, Slovenian Forestry Institute, Vecna pot 2, SI-1000 Ljubljana, Slovenia

[2]Department of Environmental Sciences, Jožef Stefan Institute, Jamova 39, SI-1000 Ljubljana, Slovenia

[3]Department of Agronomy, Biotechnical Faculty, University of Ljubljana, Jamnikarjeva 101, SI-1000 Ljubljana, Slovenia

***Corresponding author:** E-mail: jozica.gricar@gozdis.si, Phone: +386 1 200 78 53

Article Type: Original Research

Running Title: Post-fire effects on *Quercus pubescens*

Author contributions All authors conceived and designed the work; ML and PH collected the samples; JG and PH carried out anatomical analyses; DV and ML performed photosynthetic measurements; MF set up the infrastructure in the field; NO and BK carried out the stable carbon isotope composition analyses; KE performed the statistical analyses and prepared the figures and tables; JG and DV wrote the manuscript; all authors critically revised the manuscript; all authors approved the final version of the manuscript to be published.

Conflict of Interest: The authors declare that they have no conflict of interest.

Key words: pubescent oak, cambium, radial growth, xylem, phloem, anatomy, sub-Mediterranean

Abstract

An increased frequency of fire events on the Slovenian Karst is in line with future climate-change scenarios for drought-prone environments worldwide. It is therefore of the utmost importance to better understand tree-fire-climate interactions for predicting the impact of changing environment on tree functioning. To this purpose, we studied the post-fire effects on leaf development, leaf carbon isotope composition ($\delta^{13}C$), radial growth patterns and the xylem and phloem anatomy in undamaged (H-trees) and fire-damaged trees (F-trees) of *Q. pubescens* with good re-sprouting ability in spring 2017, the growing season after a rangeland fire in August 2016. We found that the fully developed canopy of F-trees reached only half of the LAI values measured in H-trees. Throughout the season, F-trees were characterised by higher water potential and stomatal conductivity and achieved higher photosynthetic rates compared to unburnt H-trees. The foliage of F-trees had more negative $\delta^{13}C$ values than those of H-trees. This reflects that F-trees less frequently meet stomatal limitations due to reduced transpirational area and more favourable leaf-to-root ratio. In addition, the growth of leaves in F-trees relied more on the recent photosynthates than on reserves due to the fire disturbed starch accumulation in the previous season. Cambial production stopped 3 weeks later in F-trees, resulting in 60 % and 22 % wider xylem and phloem increments, respectively. A novel approach by including phloem anatomy in the analyses revealed that fire caused changes in conduit dimensions in the early phloem but not in the earlywood. However, premature formation of the tyloses in the earlywood vessels of the youngest two xylem increments in F-trees implies that xylem hydraulic integrity was also affected by heat. Analyses of secondary tissues showed that although xylem and phloem tissues are interlinked changes in their transport systems due to heat damage are not necessarily coordinated.

Introduction

The landscape history of Mediterranean-type ecosystems shows strong changes of its use; from intensive and extensive land use in the past to increasing abandonment in recent decades (Pausas 2006). Land abandonment results in increasing the cover of early-succession woody species, which is allegedly one of the main reasons for the increased frequency of fire events (Pausas 2006). Such a situation is also characteristic of the Slovenian karst (Kaligarič and Ivajnšič 2014), which is one of the most fire-endangered areas in the country, with an increasing frequency of fire events and the extent of burned areas since 2003 (Veble and Brečko Grubar 2016). The great majority of the fires here are caused by infrastructure, e.g., trains, which throw sparks along the track, or human negligence. The periods with the highest frequency of fire events are February–March and July–August, with a higher extent of burnt areas coinciding with the latter period, characterised by long dry periods, rainfall shortage and high temperature (Veble and Brečko Grubar 2016). Since fire risks are increasing in the Mediterranean also because of climate change associated with increased intensity and frequency of heat waves and prolonged droughts (Schröter et al. 2005), the impact of such changes on forest ecosystems deserves deeper investigation.

Fire can directly harm trees causing heat-induced injuries, tissue necrosis. These can lead to the death of plant parts, organs or, when fire is particularly destructive, to mortality of a tree. The affected tree part, extent and severity of these first-order fire effects depend very much on the type of the fire, its intensity, and on the heat transfer into tissues in roots, stem and crown (Bär et al. 2019). Nonlethal heat injuries can trigger second-order effects, impaired carbon and water balance and increased susceptibility to biotic stress (Michaletz and Johnson 2007, Bär et al. 2019).

71 Vegetation in fire-prone ecosystems has evolved traits contributing to plant persistence
72 and regeneration after fire (Paula et al. 2009). Among others there are ones limiting heat transfer
73 to most vital tissues. In trees, thick dead bark provides strong heat insulation to prevent injuries of
74 the inner tissues and preserves functionality of phloem, i.e. assimilate allocation and storage, and
75 activity of vascular cambium, i.e. secondary growth (Pausas 2015). However, when fire intensity
76 exceeds bark insulation capability critical necrosis temperatures can develop not only there but
77 also in the underlying xylem. Its hydraulic function can be impaired due to an enhanced risk for
78 cavitation and heat induced structural alterations. Fire can cause changes in the fine wood
79 structure, such as pit architecture, e.g., porosity of pit membranes, or cell wall structure
80 (Michaletz et al. 2012, Bär et al. 2018). In ring-porous *Castanea sativa,* tyloses, which block
81 vessels lumen, were formed in response to fire occurring during the growing season (Bigio et al.
82 2010). Hydraulic integrity can be impaired until dysfunctional sapwood area is completely
83 replaced. The recovery is faster in species with few active xylem rings, such as oaks, where
84 annual xylem increment represents a large portion of the sapwood area. Battipaglia et al. (2014)
85 showed such a reaction for *Pinus halepensis* where a decrease in radial growth and in relative
86 conductivity in the first year after the fire was followed by complete recovery. However,
87 frequently wood-anatomical post-fire effects may appear several years following fire, due to
88 cambium dysfunction, reduced carbohydrate pools and stomatal limitations of photosynthesis,
89 induced by hydraulic effects. When fire induced carbon starvation and hydraulic dysfunction are
90 too severe, they can lead to tree mortality, most commonly co-induced by other stress factors
91 such as drought or pest attack (Michaletz 2018, Bar et al. 2019).

92 In terms of post-fire tree mortality, the degree of crown injury and ability for foliage
93 recovery is also relevant (Catry et al. 2010). Sufficient leaf area is needed to cover the demand for

94 carbohydrates and maintain favourable carbon balance. Mediterranean *Quercus* species can
95 resprout efficiently after fire and regenerate from seeds (Pausas 2006). However, the intervals
96 between recurrent fires were shown to be the main determinant of post-fire resilience, due to their
97 direct effect on mortality, selection and replacement of plant populations (Schaffhauser et al.
98 2012). *Quercus pubescens* thrives successfully only in mixed forest stands or woodlands with low
99 fire recurrence, where seed dispersal is efficient and seedlings can germinate in the shade.
100 Climate change and increased fire frequency may have a severe impact on its post-fire survival
101 and regeneration capacity (Curt et al. 2009). Trees weakened by fire are particularly vulnerable to
102 periods of drought in the years that follow fire events (Catry et al. 2010). It is therefore important
103 to understand tree-fire-climate interactions for predicting the impact of changing environment on
104 tree functioning. Despite several publications on the post-fire effect on different tree properties,
105 such as xylem structure and hydraulics, intra-annual patterns of radial growth were not examined
106 in these studies. In particular, the response of phloem is poorly understood in this respect
107 although, as the living tissue located directly under the dead bark, it is often damaged by fire and
108 its injuries seriously impair long-distance source-to-sink transport of carbohydrates (Hölttä et al.
109 2014).

110 Because of the increased frequency of fire events on the Slovenian karst (Veble and
111 Brečko Grubar 2016), we investigated the effect of this disturbance event on *Q. pubescens,* a
112 dominant tree species in this region. In the period 7–10 August 2016, a forest fire occurred and
113 burnt about 460 ha of the area (Zavod za gozdove Slovenije 2017). Since cambial cell production
114 of *Quercus pubescens* had finished by that date (Gričar et al. 2018), it did not affect radial growth
115 in the current growing season, but we assumed that a post-fire effect would be traceable in the
116 following growing season and would affect: (i) leaf development and functioning, (ii) stem radial

117 growth dynamics and (iii) xylem and phloem anatomy in different tree parts. To test this
118 hypothesis, we selected two groups of *Q. pubescens*, undamaged (H-trees) and trees damaged by
119 the fire (F-trees) and performed eco-physiological, stable carbon isotope and anatomical analyses.
120
121 **Material and methods**
122 ***Study site characteristics***
123 The study site was located on the Podgorski Kras (45°32'56.3"N, 13°54'36.1"E, 430 m a.s.l.),
124 which belongs to the karstic region in SW Slovenia. Since the abandonment of the area about 30
125 years ago, it has been overgrown by various woody plant species. One of the dominant tree
126 species is pubescent oak (*Quercus pubescens* Willd.), which grows either in patches or solitary.
127 The climate is sub-Mediterranean, with typical fairly harsh winters (T_{Jan} = 2.8°C for the period
128 1992–2017) and frequent dry and hot summers (T_{Jul} = 21.5°C for the period 1992–2017). In 2017,
129 the average annual air temperature was 12.2°C (T_{Jan} = –0.4°C, T_{Aug} = 22.8°C), the total annual
130 precipitation was 1505 mm. The data were recorded from the nearby Kozina climate station
131 belonging to the Slovenian Environment Agency (ARSO) (Figure 1). Despite relatively high
132 annual precipitation (P = 1300 mm for the period 1992–2017), shallow soil and regular wind
133 diminish its impact, resulting in a large proportion of deep percolation loss of soil water and,
134 consequently, frequent drought events, particularly during the summer period (Ferlan et al. 2016).
135 The bedrock on the plot is rendzic leptosol on paleogenic limestone.
136
137 [Figure 1]
138

Tree selection and leaf analysis

A forest fire occurred at the site from 7–10 August 2016; high-spread low intensity fire damaged the understorey aboveground biomass and, at the same time, caused significant scorching of *Q. pubescens* crowns (Zavod za gozdove Slovenije 2017). The leaves of trees, up to a height of ca. 7 m, dried and died but were mostly not burnt and remained on the trees. Small twigs were also damaged. The fire effects, however, were not uniform. Since the forest stand is very sparse, certain parts of the forest fire area suffered little or no damage. The fact that some trees were left intact enabled us direct assessment of post-fire effects on tree growth. In burnt trees that had lost a considerable part of their leaf area re-spouting of new shoots occurred in September 2016, after the first autumn rains. In October 2016, two groups of six pubescent oaks (*Quercus pubescens*) 55 ± 5 years old, similar in their DBH (20 ± 1.5 cm), height (10 ± 1.5 m) and bark thickness at the breast height (1.53 ± 0.29 cm), were selected for the study. In the group of H-trees, trees with no visible heat damage on the stem bark or crown were assigned. No post fire re-sprouting was detected in autumn 2016. In addition, herb and shrub layers were not affected by the fire. F-trees were chosen on areas where herb and shrub layers were damaged and tree level considerably affected due to heat exposure. The group of F-trees consisted of trees that had survived but were damaged by the fire. Signs of damage were visible as stem-bark chars extended up to 2 m above the ground and the presence of autumn shoots. F-trees suffered more than 95 % of leaf-loss based on drone aerial photo estimation. In March 2017, we removed a small portion of dead bark to make sure that heat exposure had not caused necrosis of living cells (i.e., inner phloem and cambium). This would have prevented phloem functioning and the radial growth of trees and thus limit their survival and consequently their suitability for the study. The assessment was done on the basis of visual observation of the colour and moisture of the inner living phloem tissue and

cambial region. If the tissue appeared dry to touch, with a dark brown colour, we concluded that it died. These trees were not considered for the sampling. If the tissue beneath the dead bark layers was moist, with a dark yellowish-red/pink colour, we concluded that damage of the stem was not too severe to cause necrosis of the living tissues. These trees were selected for the study and were assigned to F group.

In 2017, we performed leaf phenological observations, leaf area index (LAI) measurements, carbon isotope composition ($\delta^{13}C$ analyses), leaf gas-exchange and water potential measurements for each group of trees. Leaf phenology was observed on all oaks at 7–10-day intervals from March until November. In particular, we focused on the period from budburst to full leaf unfolding, i.e., March–May. To document leaf development, images of a selected crown part were captured on each sampling date with a digital camera. The methodology is described in detail in Gričar et al. (2017). At the same time, LAI, the one-sided leaf surface area per ground surface area (m^2m^{-2}), was measured for each group of oaks with a LAI-2200 Plant Canopy Analyzer (LI-COR Inc., USA). LAI measurements were performed in several transects in the small woodland patches in which the selected trees were growing. Mean LAI per tree group was calculated for each measurement term, i.e. ,7–10-day interval (LAI-2200 Instruction Manual 2012, for details see Lavrič et al. (2017)).

At the same time, leaves for the $\delta^{13}C$ analysis were sampled from each assigned individual tree in both groups at the sun exposed southern part of the crown at 4–5 m above the ground. In the laboratory, the leaves were dried in the oven, grounded to fine dust using ball grind mill. Leaves from the same group of trees were pooled to perform the $\delta^{13}C$ analysis. Altogether 50 samples were analysed; that is 25 samples for each tree group. A known mass of each dry leaf sample was weighed in a tin capsule. Stable isotope ratios of carbon ($^{13}C/^{12}C$) measurements were

185 performed on a 20–20 continuous flow IRMS (Europa Scientific, Crew, UK) with an ANCA-SL
186 solid-liquid preparation module. The stable carbon isotopic values are expressed in the delta
187 notation, $\delta^{13}C$, as the deviation, in parts per million (‰), from the Vienna Pee Dee Belemnite
188 (VPDB) standard for carbon. Analyses were calibrated against certified reference materials:
189 IAEA-CH-3 (cellulose), SERCON Protein (Casein) OAS and SERCON Wheat Flour OAS values
190 of −24.72 ± 0.05‰, −26.98 ± 0.13‰, and −27.21 ± 0.13‰, respectively. The precision of the
191 measurements for bulk material was ±0.2‰.

192

193 ***Leaf gas exchange, leaf water potential***

194 Leaf measurements were taken four times during the growing season, covering different stages of
195 radial growth and periods with different water availability: 21 June, 18 July (in the period of
196 latewood formation), 8 August (at the cessation of cambial activity, drought period) and 24
197 August (in the period of wall formation of terminal latewood cells, drought period). Fully
198 developed sun exposed leaves from the southern part of the crown were measured by using two
199 LI-6400 XT portable photosynthesis systems (LI-COR, Lincoln, USA). Measurements were
200 taken simultaneously for the two tree groups, from 9 to 11 a.m., at a constant reference CO_2
201 concentration (400 μmol mol^{-1}) and photon flux density (1500 μm mol m^{-2} s^{-1}), controlling
202 temperature and water vapour deficit at the ambient level (targeting to average for measuring
203 time with respect to daily weather conditions). Six leaves each from three trees were measured
204 per group. Net photosynthesis (A), transpiration (E), stomatal conductance (g_s) and intercellular
205 leaf CO_2 concentration (C_i) were recorded when steady state conditions had been reached.

206 The measured leaves were collected and the chlorophyll content was determined by
207 SPAD (Konica-Minolta Sensing Inc., Osaka, Japan). Homogeneity in the light exposure of the

measured leaves was tested by assessing specific leaf area, after the leaves had been scanned (area measurements), dried and weighed in the lab. The same leaves were analysed for isotopic composition.

On-site measurements of midday (Ψ_{midday}) and predawn water potential ($\Psi_{predawn}$) were determined in the leaves, similar to those measured by Li6400, using the pressure chamber technique (Scholander, Hemmingsen, Hammel & Bradstreet, 1964; chamber 3005–1223, Soil Moisture Equipment Corp., Goleta, USA). Three leaves each from three trees were sampled for each tree group.

Xylem and phloem tissue analysis

For analysis of xylem and phloem formation, microcores were collected at weekly intervals from end-March until mid-October 2017, using a Trephor tool (Rossi et al. 2006). The samples were taken at 0.7–1.7 m above the ground following a helical pattern up the stem and separated by 3–5 cm in order to avoid wound effects. Each microcore contained non-collapsed and collapsed phloem, cambium and at least three of the last-formed xylem rings. For xylem and phloem anatomy analysis, microcores were collected in November, when current annual phloem and xylem increments were fully developed. In this case, the samples were taken from three different tree-parts: two locations from the stem, 1.5 m and 3 m above the ground and one from a branch, 3 m from the apex. The sampled branches, with diameters at the sampling locations of 6.0±1.1 cm, were located approximately 3 m above the ground. In F-trees, sampling at stem below 2 m above the ground was performed on the scorched area and above that height on the unburnt stem part. Immediately after removal from the trees, the samples were fixed in ethanol-formalin acetic acid

230 solution (FAA) and further processed in the laboratory for preparation of transverse sections
231 stained with safranin and astra blue for histometrical analysis (see Gričar et al. 2017 for details).

232 On the sections intended for radial growth analysis: (1) the number of cells in the
233 cambium was counted and (2) the widths of currently formed xylem and phloem increments
234 along three radial files were measured and then averaged. We assessed the following
235 developmental phases of xylem and phloem formation, expressed in days of the year (DOY): (1)
236 onset /end of cambial cell production; (2) maximum rates of xylem and phloem cell production;
237 (3) transition from earlywood to latewood and from early to late phloem and (4) cessation of
238 wood formation. The definitions of each phase are described in Gričar et al. (2017). We analysed
239 the hydraulic architecture in earlywood and early phloem in completely developed xylem and
240 phloem increments of samples taken at three positions in a tree. In the case of xylem, we assessed
241 the fire effect on wood hydraulics by analysing the anatomy of the latest three increments (2015-
242 2017), i.e., formed before and after the fire. Specifically, the following earlywood vessel
243 parameters were analysed and mean values calculated: tangential diameter (MVD), area (MVA)
244 and density (VD: number of cells / 1 mm^2). Earlywood vessel parameters were analysed for the
245 first ring of vessels and for all earlywood vessels. In phloem, we analysed the youngest phloem
246 increment of 2017. The tangential diameter (MSD) and area (MSA) of 30 randomly selected
247 sieve tubes of early phloem were measured and mean values calculated.

248

249 ***Statistical data analysis***

250 Statistical data analyses were different for different groups of tree functioning parameters. For
251 wood and phloem formation milestones, one-way ANOVA was used to compare the two groups
252 of trees (H and F). For phloem anatomy parameters, factorial ANOVA was used to test for

253 significance of tree group (2 levels) and tree part (3 levels). For xylem anatomy, a linear mixed
254 model was used, with tree group, tree part and year as fixed factors and tree as random factor.
255 Similarly, linear mixed models were developed for leaf physiology parameters with tree group
256 and day of year as fixed factors and leaf and tree as random factors (leaf nested within tree).

257 The Gompertz function was fitted to the increments of xylem and phloem widths for each
258 tree group separately (Rossi et al. 2003). Model fits were evaluated by computing mean absolute
259 error and Efron's pseudo-R^2 (calculated as one minus the ratio between the sum of squared model
260 residuals and the sum of total variability). To investigate the differences between tree groups in
261 xylem and phloem growth, the joint Gompertz model for combined data of all tree groups was
262 compared with a model with tree groups being the fixed cofactor. The comparison was made
263 using a partial F-test.

264 In all cases, the assumption of normality was assessed graphically (Q-Q plot) and
265 homogeneity of variance was tested using the Levene test. When assumptions were violated,
266 Box-Cox transformation was used for variance stabilisation and greater normality in data
267 distribution. In all tests, a 0.05 significance level was used. Data were analysed using R
268 environment (package nlme) (R Core Team 2018).

269

270 **Results**

271 ***Leaf phenology and carbon isotope composition***

272 Spring leaf phenology was comparable in the two tree groups. LAI values followed leaf
273 development; although the values were higher in H-trees in all cases (Figure 2). Buds started to
274 open in the first half of April (DOY 105.9 ± 5.4), followed by first leaf emergence in the second

part of April. In mid-April, the average LAI values were 0.42 ± 0.12 m^2m^{-2} for H-trees and 0.25 ± 0.10 m^2m^{-2} for F-trees. Full leaf unfolding occurred by mid-May (DOY 138–140). At that time, the LAI values were 1.86 ± 0.39 m^2m^{-2} for H-trees and 1.00 ± 0.19 m^2m^{-2} for F-trees. The period from bud opening to full leaf unfolding lasted on average 32 days.

The average $\delta^{13}C$ values in leaves varied with respect to the tree group and the sampling time (Figure 2). The highest mean $\delta^{13}C$ values were found in the second half of April, at the time of budburst and first leaf emergence, and ranged from –24.9‰ to –24.2‰ in H-trees and from –26.9‰ to –25.9‰ in F-trees. In the period of leaf development, which was completed by the third week of May, the values decreased to –28 and –27‰ in H-trees and to –29 and –28‰ in F-trees. From this period onward, the values were fairly stable for both tree groups until abundant leaf colouring at the beginning of October, when we completed sampling. In the 2017 growing season, therefore, $\delta^{13}C$ values were generally lower in F-trees; on average 2.1‰ lower during leaf development and 0.8‰ in the period of full leaf unfolding.

[Figure 2]

Leaf physiology

Over the course of the season, F and H trees differed in many ecophysiological parameters measured on the leaf level (Table 1, 2). Both predawn and midday water potential revealed higher water availability in F-trees than in H-trees with DOY 220 being an exception for Ψ_{midday}. Differences in water balance were further reflected in the higher stomatal conductivity of F-trees. These were not uniformly translated into transpiration rates, however. The differences between *E*

297 of F and H trees were inconsistent. Net photosynthesis (*A*) was higher in H trees at the first and
298 last measurements (DOY 172, 236), but the opposite was found for mid-season. In July (DOY
299 199), the *A* of F-trees largely exceeded that of H-trees.

300

301 [Table 1]

302

303 [Table 2]

304

305 ***Radial stem growth***

306 Wood and phloem formation dynamics and milestones in H-trees and F-trees are presented in
307 Figure 3 and Table 3. The fire in summer 2016 had an impact on radial stem growth in *Q.*
308 *pubescens* in 2017; especially in the period of latewood formation. Radial growth started at the
309 end of March in both tree groups but it stopped on average 3 weeks later in F-trees. In
310 combination with the higher rate of cambial cell production in F-trees, this resulted in around 60
311 % and 22 % wider xylem and phloem increments, respectively (Figure 3, Table 3). Thus,
312 earlywood and latewood were about 45 % and 75 %, respectively, wider in F-trees. In addition,
313 the fire affected the timing of tylose appearance in earlywood vessels of 2016 and 2017; they
314 were formed about 3 weeks earlier in F-trees than in H-trees; i.e., at the beginning of April and at
315 the beginning of August, respectively. In phloem, early phloem and late phloem were about 18 %
316 and 50 %, respectively, wider in F-trees.

317

[Figure 3]

[Table 3]

Xylem and phloem anatomies in different tree parts

In all cases, xylem and phloem anatomies significantly differed between stem and branch; annual increments were wider and earlywood/ early phloem conduits were bigger in the stem (Figure 4, 5, Table 4). Furthermore, the annual increment widths of xylem and phloem differed between the two groups; in all cases, the increments were wider in F-trees. Because radial growth had finished by the time of the fire in August 2016, the increments were not affected in that year; however, the widths of 2017 were reduced. The relative decrease in the widths from 2016 to 2017 was more pronounced in H-trees (about 40 %) than in F-trees (about 20 %). In terms of conduit size in the branch and stem, earlywood vessels were smaller and their density higher in the branch (Figure 4, Table 4). Similarly, early phloem sieve tubes were smaller in the branch than in the stem. No distinctive post-fire effect was detected in the size of earlywood conduits in H- and F-trees. In contrast, phloem conduit size significantly differed between H- and F-trees (Figure 5, Table 4), with sieve tubes size being bigger in H-trees. Thus, compared to F-trees, sieve tube areas in H-trees were about 21.4 % and 28.4 % bigger in stem and branch, respectively.

[Figure 4]

[Figure 5]

[Table 4]

Discussion

It was shown in our research, that even though the first-order fire effects were limited to damage of foliage, and caused no necrosis of cambium/phloem or injuries of roots, they influenced tree carbon and water balance, which was translated into changed growth and developmental patterns in *Q. pubescens*. The reduction of *Q. pubescens* crown leaf area contributed to i) probably reduced reserves of carbohydrates produced in the season of disturbance; to ii) improved water relations, iii) enhanced leaf photosynthesis (related to effect ii)) and iv) changed secondary stem growth. Phloem and xylem were not equally affected by the fire; it caused changes in the phloem conduit properties, while the size of earlywood vessels remained unmodified. However, premature formation of the tyloses in the earlywood vessels of the previous and current xylem increments in F-trees implies that xylem hydraulic integrity was also affected by heat.

Leaf development and physiology

As expected, LAI values increased with leaf development, which occurred in the period from mid-April until mid-May. In all cases, LAI values were higher in H-trees, with an average difference of 1.0 m^2m^{-2} at the time of full leaf unfolding. The lower LAI values of F-trees clearly indicate a post-fire effect on leaf development. Average LAI values of fully developed crowns of H-trees (2.0 m^2m^{-2}) are in line with our previous measurements on solitary *Q. pubescens* at this study site (2.2 m^2m^{-2}, Lavrič et al. 2017).

362 Reductions in total leaf area after disturbance such as fire are known to influence the
363 carbon and water balance of trees. Burnt trees have less foliage per unit of sapwood and may
364 have more foliage distributed at lower heights, both of which significantly influence water
365 transport to the canopy. Due to the higher root to shoot ratio and ratio of sapwood to leaf area,
366 leaves have better access to water. In addition, water supply could be improved due to reduced
367 competition from herb and shrub layer which was more affected by fire (heat induced injuries).
368 Increased water availability supports higher stomatal conductance and photosynthetic rates. Such
369 trees can avoid stomatal limitations under progressing drought longer (Fleck et al. 1998, Nolan et
370 al. 2014, Renninger et al. 2014, Bär et al. 2019). Our results accord well with these general
371 observations. Throughout the season, F-trees were characterised by higher water potential and
372 stomatal conductivity than unburnt H-trees. In mid-summer (DOY 199 and 220), the high g_s
373 supported the supply of CO_2 into the leaves of F-trees and, as a consequence, they achieved
374 higher photosynthetic rates than H-trees. On the other hand, the opposite was true in June and late
375 August, when the A of H-trees slightly exceeded the A of F-trees. Fleck et al. (1998) reported that
376 the fire treatment effects on leaf physiology of *Q. ilex*, i.e., increase of A and g_s, were enhanced in
377 the period when plants were subjected to high temperature, irradiance and VPD. In their study,
378 re-sprouts did not show midday depressions of A and g_s, and preserved high photochemical
379 efficiency, while unburnt trees coped with stomatal limitations of photosynthesis and
380 photoinhibition.

381 We found that $\delta^{13}C$ values in young developing leaves were less negative in both groups
382 compared with mature leaves, which is in line with earlier observations in *Q. pubescens*
383 (Damesin et al. 1998). Furthermore, the $\delta^{13}C$ values of mature leaves (H-trees: from –28 to –
384 27‰; F-trees: from –29 to –28‰) are in accordance with the literature data (O'Leary 1988,

385 Damesin et al. 1998). In *Q. pubescens*, most $\delta^{13}C$ and biochemical changes occur during leaf
386 expansion, which partly illustrates the major decrease of $\delta^{13}C$ during leaf growth (Damesin et al.
387 1998). The isotope content of a leaf gives an insight into its carbon gains and losses (Damesin
388 and Lelarge 2003). Damesin et al. (1998) explained $\delta^{13}C$ values of a mature leaf of *Q. pubescens*
389 with three components: (i) $\delta^{13}C$ in the initial phase of leaf construction, which depends on stored
390 carbon; (ii) $\delta^{13}C$ of carbon assimilated during leaf expansion and (iii) $\delta^{13}C$ of assimilates that are
391 involved in the turnover of leaf matter. Since photosynthesis of young developing leaves in
392 deciduous oaks does not suffice for a positive leaf carbon balance, reserves stored from the
393 previous growing seasons are involved in growth. Starch, which forms part of these reserves, has
394 higher $\delta^{13}C$ values than soluble sugars (Brugnoli et al. 1988). During conversion from
395 heterotrophy to autotrophy, assimilates with lower $\delta^{13}C$ values are built into leaves (Damesin and
396 Lelarge 2003). In addition, changes in the relative proportion and activity of PEP carboxylase and
397 Rubisco in leaves are considered to contribute to the decrease in $\delta^{13}C$ values (Terwilliger et al.
398 2001).

399 We found that during the entire growing season, $\delta^{13}C$ values were more negative in the
400 leaves of F-trees. This could be attributed to their higher dependence on recent carbohydrates
401 derived directly from photosynthesis. High demand is also reflected by high photosynthetic rates.
402 On the other hand, the growth of the unburnt, H-trees may be supported to a larger extent by
403 carbohydrates produced/stored in the late summer and autumn of the previous year. The burnt
404 trees lost part of the leaves and possibly also fine roots at the beginning of August 2016, just after
405 the start of the starch accumulation period (Gričar et al. 2018). Due to reduced reserves of
406 carbohydrates, which can decrease after a fire not only in the stem but also in the coarse roots

(Varner et al. 2009), the yearly carbon balance of the trees was affected. This also influenced the carbon allocation patterns in the next season.

Another contribution to more negative $\delta^{13}C$ values of F-trees is related to stomatal functioning. Our gas exchange measurements indicated that F-trees operated with high stomatal conductivity, which brings a high CO_2 concentration in the internal space of the leaf and supports strong discrimination against ^{13}C. Water potential and g_s reveal that H-trees more easily meet the stomatal limitations of photosynthesis. The consequence of lower g_s is weaker discrimination, yielding less negative $\delta^{13}C$ values of the foliage (Pate 2001).

Radial growth in Q. pubescens after a fire event

Comparison of the xylem increments formed in 2016 and 2017 showed that the widths in the latter year were reduced by 40 % in H-trees and 20 % in F-trees. Battipaglia et al. (2014) reported that a decrease in radial growth of *P. halepensis* was noted in the year after a fire event, but the trees later recovered, suggesting that the heat-related damage is not permanent. Reduced xylem increments in a year after a fire may indicate a carbon saving strategy of trees in response to various disturbances (Deslauriers et al. 2015). Saving storage reserves would enable trees to mitigate harmful events related to any other stressors (Pérez-de-Lis et al. 2016), such as, for example, summer drought periods, which are frequent in the study area.

However, since xylem increments were wider in F-trees in all three analysed years 2015–2017 it is not possible to attribute the differences between H- and F-trees in radial growth dynamics in 2017 solely to the fire event in the previous year. In fact, xylogenesis data in *Q. pubescens* in 2014–2016 from the same location (Gričar et al. 2017, 2108, Lavrič et al. 2017)

showed that radial growth in H-trees stopped 19–27 days earlier than in the previous years, while the cessation of cell production in F-trees was comparable with the previous data. Weather conditions in 2017 would explain premature cessation of cambial cell production in H-trees. Although 16 % more rainfall was recorded in 2017 compared to the 24-year average (1992–2016), the period May–July was dry with about 43 % less precipitation, which most probably negatively affected the duration of radial growth in H-trees. Gas exchange data revealed that in July (DOY 199) due to higher water availability F-trees operated at high stomatal conductivity achieving high photosynthetic rates, while stomatal g_s and A decreased in H-trees. Stomatal limitation of photosynthesis and reduced carbohydrate pools could lead to premature cessation of xylogenesis in these trees. On the other hand, it is to presume that in this dry period of the year F-trees can build more carbohydrates supporting radial growth of the stem, i.e. prolonging xylogenesis. This could help to restoration of hydraulic function which had been affected by premature, fire-induced tylose formation in the earlywood vessels of the previous and current xylem increments (see next sub-chapter 'Post-fire effect on earlywood conduits' for a more detailed explanation).

There have been no similar studies on the post-fire effect on the width of the phloem increment in other tree species. However, a comparison of the widths with our previous studies (Gričar et al. 2017, 2018, Lavrič et al. 2017) revealed that the rings of H-trees were on average 18 %–38 % narrower than in 2014, 2015 and 2016. In contrast, the widths of F-trees were comparable to the former data, confirming the above mentioned assumption on the importance of rebuilding a translocation pathway in the phloem and therefore maintaining secondary growth despite adverse weather conditions.

Post-fire effect on earlywood conduits

Size of earlywood conduits was not affected by the fire of the previous summer. This could be attributed to favourable weather conditions in spring 2017, especially in April, a crucial month for earlywood vessel formation, because it is well supplied with precipitation. Vessel characteristics have been reported to depend mainly on two physiologically decisive periods for their development: autumn of the previous year and early spring of the current year (Eckstein 2004). At the end of the previous growing season, carbohydrates are formed and stored in parenchyma cells (Atkinson and Denne 1988, Barbaroux and Bréda 2002). These reserves are used for earlywood vessel formation the following year, which occurs in ring-porous *Q. pubescens* before full leaf development (Zweifel et al. 2006). Vessel expansion and wall formation occur in early spring; weather conditions in this period therefore mainly determine its final size (e.g., Fonti and García-González 2004). In particular, water availability, which affects turgor pressure in the cells, is important for cell dimensions (Hölttä et al. 2010). However, Rosell et al. (2017) recently pointed out that, globally, tree size and crown size explain vessel diameter variation much more than climate. Taller plants can thus be found in moister areas, with wider vessels at the stem base due to basipetal vessel widening.

Narrower conduits in the branches of *Q. pubescens* support a universal conduit tapering in xylem and phloem towards the tree apex (Anfodillo et al. 2012, Olson et al. 2014, Jyske and Hölttä 2015), partly to compensate for the effect of tree height on hydraulic resistance (Petit et al. 2010). In addition to the size of the conduits in xylem, vessel density, which is inversely proportional to vessel size, is considered to be important for whole-tree conductance (Petit et al. 2010). This pattern was also confirmed in our present and past studies in *Q. pubescens* (Gričar et al. 2017); earlywood vessels decreased in size and increased in number towards the tree apex.

475 Vessel characteristics are regulated by hormones, in particular by a decrease in auxin
476 concentration in a basipetal direction (Aloni 2015). Because of rapid differentiation in the crown
477 with high auxin concentrations, vessels are narrow and numerous, whereas low auxin
478 concentrations in the lower parts of the tree slow down the differentiation process. This allows
479 more time for vessel expansion, which results in wider and fewer vessels (Aloni and
480 Zimmermann 1983).

481 Although no differences were found in the size of earlywood vessel between H- and F-
482 trees, tyloses, which blocked vessels' lumen, appeared about 3 weeks earlier in the earlywood
483 vessels of F-trees. In these trees, most of the earlywood vessels formed in 2016 were blocked
484 with tyloses at the beginning of April and earlywood vessels of 2017 at the beginning of August.
485 Similarly, Bigio et al. (2010) noted that fire during the growing season induced tylose formation
486 in *C. sativa*. Under normal conditions, wide earlywood vessels in ring-porous species become
487 blocked with tyloses by the end of the current growing season (Kitin and Funada 2016).
488 However, tylose formation can be provoked by various abiotic and biotic stressors, such as
489 flooding, freezing, mechanical wounding, crown damage or pathogen infection. Since jasmonates
490 and ethylene are the key molecular triggers of tyloses (Leśniewska et al. 2017, McElrone et al.
491 2010), it is to presume that hormonal signal, possibly deriving from scorched crown, contributes
492 to the observed response.

493 In certain part of the season premature presence of tyloses negatively affected the
494 hydraulic conductivity of F-trees. This was compensated by prolonged xylogenesis resulting in
495 wider xylem rings with a larger proportion of latewood. Since the small-diameter latewood
496 vessels may remain functional for many years, a combination of wide and narrow vessels ensures
497 efficiency and safety of the water transport (Kitin and Funada 2016). Thus, in the case of earlier

498 formation of tyloses in earlywood vessels, small-diameter latewood vessels are important for
499 water conduction despite their much lower conducting capacity. In ring-porous pubescent oak,
500 more cavitation-resistant latewood vessels serve as a high-safety but low-efficiency back-up
501 system in the case of stressful events and may function to prevent complete transport failure
502 (Taneda and Sperry 2008).

503

504 ***Post-fire effect on phloem anatomy***

505 In F-trees, the phloem conduits were smaller, while the phloem increment was wider. In
506 particular, late phloem was about 50 % wider in F-trees than in H-trees. Late phloem sieve tubes
507 in oak are generally narrower than those of early phloem (Gričar et al. 2015). However, late
508 phloem contains larger amounts of axial parenchyma, acting as a storage organ for non-structural
509 carbohydrates (Barbaroux and Bréda 2002, Plavcová et al. 2016). In deciduous trees that shed
510 their leaves seasonally, storage reserves are important for their maintenance during the leafless
511 season and for coping with stresses and disturbances, such as drought, fire and herbivores
512 (Martínez-Vilalta et al. 2016). Trees thus need to coordinate the use of the limited supply of
513 reserves for metabolic and structural demands (Dietze et al. 2014). Key morphological traits of
514 tree resistance to disturbance events are thick dead bark for inner living tissue protection and
515 storage reserves for its successful recovery (Catry et al. 2010). These reserves are also used for a
516 second growth of foliage or re-sprouting in the case of crown fire damage (Dietze et al. 2014).
517 This may cause a loss in carbon production, which can result in its shortage for growth, storage
518 and defence functions in a tree (Deslauriers et al. 2015). It can be assumed that depleted amounts
519 of reserves could at some point compromise tree functioning, which could even lead to tree
520 mortality (Michaletz et al. 2012). In line with this interpretation, the wider late phloem rich in

521 axial parenchyma in F-trees is likely to compensate for reserves used for new foliage in the
522 previous autumn. Furthermore, in F-trees, sieve tubes were smaller although the annual phloem
523 increment was wider, which could be a counterbalance for their smaller size. Differences in
524 phloem anatomy between the two tree groups could thus be attributed to changed foliage and
525 possible damage to older sieve tubes in F-trees. Although sieve tube functioning is generally
526 limited to the current growing season, late phloem sieve tubes formed in the previous year are
527 important for maintaining the translocation pathway for photosynthates and other biomolecules
528 from leaves, i.e. carbon source, to carbon sink sites at the onset of the growing season (Prislan et
529 al. 2018). If functional sieve tubes are damaged, rapid restoration of long-distance transport in
530 phloem is crucial for tree survival. This may explain greater differences in the phloem than in the
531 xylem anatomy. In spite of the great importance of phloem transport for tree functioning,
532 previous studies have been primarily focused on possible changes in xylem structure after fire
533 events. However, our study clearly demonstrated that, even though phloem and xylem tissues are
534 ultimately linked (Pfautsch et al. 2015), changes in their transport systems due to heat damage are
535 not necessarily coordinated. If nothing else, outer living phloem cells are much more exposed to
536 heat-impairment than inner xylem tissue; consequently, the damage is more extensive.

537

538 **Conclusions**

539 The increased frequency of fire events on the Slovenian karst that has been observed in the last
540 two decades (Veble and Brečko Grubar 2016) is in line with future climate-change scenarios for
541 drought-prone environments (IPCC 2014). Fire disturbances accompanied by drought and
542 herbivores will substantially change the carbon-water fluxes of such ecosystems. Since fires are
543 one of the most important agents of landscape change worldwide (Ferreira et al. 2019), it is

544 therefore of the utmost importance to understand better the functional and structural response, i.e.
545 ecophysiological modifications and anatomical adaptations, of trees to such disturbances (Nolan
546 et al. 2014). Heat injuries caused by a fire can trigger complex postfire mechanisms that affect the
547 physiology of trees, which are still not satisfactorily understood (Bär et al. 2019). As a result of
548 diminished radial growth, carbon accumulation in a tree is substantially reduced (Cuny et al.
549 2015). Fire associated tree mortality may change the ecosystems from carbon sink to carbon
550 source (Baldocchi 2008, Loehman et al. 2014). Unravelling the underlying mechanism of fire-
551 caused tree mortality is thus relevant for modelling carbon-water fluxes at different levels taking
552 into account also novel future climatic conditions (Hood et al. 2018). Proper counter-strategies
553 regarding the global carbon cycle will in this way be possible to develop (Bär et al. 2018).

554

555 **Acknowledgments**

556 The authors gratefully acknowledge the help of Gregor Skoberne, Urša Pečan, Jan Eržen, Boštjan
557 Zupanc, Gabrijel Leskovec and Robert Krajnc in the field and laboratory. We thank Zlatko Rojc
558 for his permission to perform the study on the plot, and Martin Cregeen for language editing. We
559 thank the editor and the reviewers for their valuable comments and suggestions, which improved
560 the quality of the paper.

561

562 **Funding**

563 This work was supported by the Slovenian Research Agency, Young Researchers Program (ML),
564 research core funding nos. P4-0085 and P4-0107, and projects J4-7203 and J4-9297.

565

566 **References**

567 Aloni R (2015) Ecophysiological implications of vascular differentiation and plant evolution.
568 Trees 29:1–16.

569 Aloni R, Zimmermann MH (1983) The control of vessel size and density along the plant axis.
570 Differentiation 24:203–208.

571 Anfodillo T, Deslauriers A, Menardi R, Tedoldi L, Petit G, Rossi S (2012) Widening of xylem
572 conduits in a conifer tree depends on the longer time of cell expansion downwards along
573 the stem. Journal of Experimental Botany 63:837–845.

574 Atkinson CJ, Denne MP (1988) Reactivation of vessel production in ash (*Fraxinus excelsior* L.)
575 Trees. Annals of Botany 61:679–688.

576 Baldocchi D (2008) Breathing' of the terrestrial biosphere: Lessons learned from a global network
577 of carbon dioxide flux measurement systems. Australian Journal of Botany 56:1-26.

578 Bär A, Michaletz ST, Mayr S (2019) Fire effects on tree physiology. New Phytologist 223:1728-
579 1741.

580 Bär A, Nardini A, Mayr S (2018) Post-fire effects in xylem hydraulics of *Picea abies*, *Pinus*
581 *sylvestris* and *Fagus sylvatica*. New Phytologist 217:1484–1493.

582 Barbaroux C, Bréda N (2002) Contrasting distribution and seasonal dynamics of carbohydrate
583 reserves in stem wood of adult ring-porous sessile oak and diffuse-porous beech trees.
584 Tree Physiology 22:1201–1210.

585 Battipaglia G, De Micco V, Fournier T, Aronne G, Carcaillet C (2014) Isotopic and anatomical
586 signals for interpreting fire-related responses in *Pinus halepensis*. Trees 28:1095–1104.

587 Bigio E, Gärtner H, Conedera M (2010) Fire-related features of wood anatomy in a sweet
588 chestnut (*Castanea sativa*) coppice in southern Switzerland. Trees 24:643–655.

589 Brugnoli E, Hubick KT, von Caemmerer S, Wong SC, Farquhar GD (1988) Correlation between
590 the carbon isotope discrimination in leaf starch and sugars of C_3 plants and the ratio of
591 intercellular and atmospheric partial pressures of carbon dioxide. Plant Physiology
592 88:1418–1424.
593 Catry FX, Rego F, Moreira F, Fernandes PM, Pausas JG (2010) Post-fire tree mortality in mixed
594 forests of central Portugal. Forest Ecology and Management 260:1184–1192.
595 Cuny HE, Rathgeber CBK, Frank D, Fonti P, Mäkinen H, Prislan P, Rossi S, del Castillo EM,
596 Campelo F, Vavrčík H, Camarero JJ, Bryukhanova MV, Jyske T, Gričar J, Gryc V, De
597 Luis M, Vieira J, Čufar K, Kirdyanov AV, Oberhuber W, Treml V, Huang J-G, Li X,
598 Swidrak I, Deslauriers A, Liang E, Nöjd P, Gruber A, Nabais C, Morin H, Krause C, King
599 G, Fournier M (2015) Woody biomass production lags stem-girth increase by over one
600 month in coniferous forests. Nature Plants 1:15160.
601 Curt T, Adra W, Borgniet L (2009) Fire-driven oak regeneration in French Mediterranean
602 ecosystems. Forest Ecology and Management 258:2127–2135.
603 Damesin C, Lelarge C (2003) Carbon isotope composition of current-year shoots from *Fagus*
604 *sylvatica* in relation to growth, respiration and use of reserves. Plant, Cell & Environment
605 26:207–219.
606 Damesin C, Rambal S, Joffre R (1998) Seasonal and annual changes in leaf $\delta^{13}C$ in two co-
607 occurring Mediterranean oaks: relations to leaf growth and drought progression.
608 Functional Ecology 12:778–785.
609 Deslauriers A, Caron L, Rossi S (2015) Carbon allocation during defoliation: testing a defense-
610 growth trade-off in balsam fir. Frontiers in Plant Science 6.
611 Dietze MC, Sala A, Carbone MS, Czimczik CI, Mantooth JA, Richardson AD, Vargas R (2014)
612 Nonstructural carbon in woody plants. Annual Review of Plant Biology 65:667–687.

613 Eckstein D (2004) Change in past environments – secrets of the tree hydrosystem. New
614 Phytologist 163:1–4.
615 Ferlan M, Eler K, Simončič P, Batič F, Vodnik D (2016) Carbon and water flux patterns of a
616 drought-prone mid-succession ecosystem developed on abandoned karst grassland.
617 Agriculture, Ecosystems & Environment 220:152–163.
618 Ferreira D, Pinho C, Brito JC, Santos X (2019) Increase of genetic diversity indicates ecological
619 opportunities in recurrent-fire landscapes for wall lizards. Scientific Reports 9:5383.
620 Fleck I, Hogan KP, Llorens L, Abadía A, Aranda X (1998) Photosynthesis and photoprotection in
621 *Quercus ilex* resprouts after fire. Tree Physiology 18:607–614.
622 Fonti P, García-González I (2004) Suitability of chestnut earlywood vessel chronologies for
623 ecological studies. New Phytologist 163:77–86.
624 Gričar J, Jagodic Š, Prislan P (2015) Structure and subsequent seasonal changes in the bark of
625 sessile oak (*Quercus petraea*). Trees 29:747–757.
626 Gričar J, Lavrič M, Ferlan M, Vodnik D, Eler K (2017) Intra-annual leaf phenology, radial
627 growth and structure of xylem and phloem in different tree parts of *Quercus pubescens*.
628 European Journal of Forest Research 136:625–637.
629 Gričar J, Zavadlav S, Jyske T, Lavrič M, Laakso T, Hafner P, Eler K, Vodnik D (2018) Effect of
630 soil water availability on intra-annual xylem and phloem formation and non-structural
631 carbohydrate pools in stem of *Quercus pubescens*. Tree Physiology 39:222–233.
632 Hölttä T, Mäkinen H, Nöjd P, Mäkelä A, Nikinmaa E (2010) A physiological model of softwood
633 cambial growth. Tree Physiology 30:1235–1252.
634 Hölttä T, Mencuccini M, Nikinmaa E (2014) Ecophysiological aspects of phloem transport in
635 trees In: Tausz M, Grulke (eds) Trees in a changing environment: Ecophysiology,
636 adaptation, and future survival. Springer, Dordrecht, pp 25–36.

637 Hood SM, Varner JM, van Mantgem P, Cansler CA (2018) Fire and tree death: understanding and
638 improving modeling of fire-induced tree mortality. Environmental Research Letters
639 13:113004.
640 IPCC (2014) Climate change 2014: synthesis report. Contribution of Working Groups I, II and III
641 to the Fifth Assessment Report of the Intergovernmental Panel on Climate Change. In:
642 Pachauri RK, Meyer LA (eds) Core Writing Team. IPCC. Geneva, Switzerland, p 151.
643 Jyske T, Hölttä T (2015) Comparison of phloem and xylem hydraulic architecture in *Picea abies*
644 stems. New Phytologist 205:102-115.
645 Kaligarič M, Ivajnšič D (2014) Vanishing landscape of the "classic" Karst: changed landscape
646 identity and projections for the future. Landscape and Urban Planning 132:148–158.
647 Kitin P, Funada R (2016) Earlywood vessels in ring-porous trees become functional for water
648 transport after bud burst and before the maturation of the current-year leaves 37:315.
649 LAI-2200 (2012) Plant Canopy Analyzer: Instruction Manual. Lincoln, NE: LI-COR.
650 Lavrič M, Eler K, Ferlan M, Vodnik D, Gričar J (2017) Chronological sequence of leaf
651 phenology, xylem and phloem formation and sap flow of *Quercus pubescens* from
652 abandoned karst grasslands. Frontiers in Plant Science 8.
653 Leśniewska J, Öhman D, Krzesłowska M, Kushwah S, Barciszewska-Pacak M, Kleczkowski LA,
654 Sundberg B, Moritz T, Mellerowicz EJ (2017) Defense Responses in Aspen with Altered
655 Pectin Methylesterase Activity Reveal the Hormonal Inducers of Tyloses. Plant
656 Physiology 173:1409-1419.
657 Loehman R, Reinhardt E, Riley K (2014) Wildland fire emissions, carbon, and climate: Seeing the
658 forest and the trees – A cross-scale assessment of wildfire and carbon dynamics in fire-
659 prone, forested ecosystems. Forest Ecology and Management 317:9-19.

660 Martínez-Vilalta J, Sala A, Asensio D, Galiano L, Hoch G, Palacio S, Piper FI, Lloret F (2016)
661 Dynamics of non-structural carbohydrates in terrestrial plants: a global synthesis.
662 Ecological Monographs 86:495–516.
663 McElrone AJ, Grant JA, Kluepfel DA (2010) The role of tyloses in crown hydraulic failure of
664 mature walnut trees afflicted by apoplexy disorder. Tree Physiology 30:761-772.
665 Michaletz ST (2018) Xylem dysfunction in fires: towards a hydraulic theory of plant responses to
666 multiple disturbance stressors. New Phytologist 217:1391–1393.
667 Michaletz ST, Johnson EA (2007) How forest fires kill trees: A review of the fundamental
668 biophysical processes. Scandinavian Journal Forest Research 22:500–515.
669 Michaletz ST, Johnson EA, Tyree MT (2012) Moving beyond the cambium necrosis hypothesis
670 of post-fire tree mortality: cavitation and deformation of xylem in forest fires. New
671 Phytologist 194:254–263.
672 Nolan RH, Mitchell PJ, Bradstock RA, Lane PNJ (2014) Structural adjustments in resprouting
673 trees drive differences in post-fire transpiration. Tree Physiology 34:123–136.
674 O'Leary MH (1988) Carbon isotopes in photosynthesis. BioScience 38:328–336.
675 Olson ME, Anfodillo T, Rosell JA, Petit G, Crivellaro A, Isnard S, León-Gómez C, Alvarado-
676 Cárdenas LO, Castorena M (2014) Universal hydraulics of the flowering plants: vessel
677 diameter scales with stem length across angiosperm lineages, habits and climates. Ecology
678 Letters 17:988–997.
679 Pate JS (2001) Carbon Isotope Discrimination and Plant Water-Use Efficiency. In: Unkovich M,
680 Pate J, McNeill A, Gibbs DJ (eds) Stable isotope techniques in the study of biological
681 processes and functioning of ecosystems. Springer Netherlands, Dordrecht, pp 19–36.
682 Paula S, Arianoutsou M, Kazanis D, Tavsanoglu Ç, Lloret F, Buhk C, Ojeda F, Luna B, Moreno
683 JM, Rodrigo A, Espelta JM, Palacio S, Fernández-Santos B, Fernandes PM, Pausas JG

(2009) Fire-related traits for plant species of the Mediterranean Basin. Ecology 90:1420-1420.

Pausas JG (2006) Simulating Mediterranean landscape pattern and vegetation dynamics under different fire regimes. Plant Ecology 187:249–259.

Pausas JG (2015) Bark thickness and fire regime. Functional Ecology 29:315–327.

Pérez-de-Lis G, García-González I, Rozas V, Olano JM (2016) Feedbacks between earlywood anatomy and non-structural carbohydrates affect spring phenology and wood production in ring-porous oaks. Biogeosciences 13:5499–5510.

Petit G, Pfautsch S, Anfodillo T, Adams MA (2010) The challenge of tree height in *Eucalyptus regnans*: when xylem tapering overcomes hydraulic resistance. New Phytologist 187:1146–1153.

Pfautsch S, Hölttä T, Mencuccini M (2015) Hydraulic functioning of tree stems—fusing ray anatomy, radial transfer and capacitance. Tree Physiology 35:706–722.

Plavcová L, Hoch G, Morris H, Ghiasi S, Jansen S (2016) The amount of parenchyma and living fibers affects storage of nonstructural carbohydrates in young stems and roots of temperate trees. American Journal of Botany 103:603–612.

Prislan P, Mrak P, Žnidaršič N, Štrus J, Humar M, Thaler N, Mrak T, Gričar J (2018) Intra-annual dynamics of phloem formation and ultrastructural changes in sieve tubes in *Fagus sylvatica*. Tree Physiology 39:262–274.

R Core Team (2018) R: a language and environment for statistical computing. R Foundation for Statistical Computing, Vienna, Austria. http://www.R-project.org/

Renninger HJ, Carlo N, Clark KL, Schäfer KVR (2014) Physiological strategies of co-occurring oaks in a water- and nutrient-limited ecosystem. Tree Physiology 34:159–173.

Rosell JA, Olson ME, Anfodillo T (2017) Scaling of xylem vessel diameter with plant size: causes, predictions, and outstanding questions. Current Forestry Reports 3:46–59.

Rossi S, Anfodillo T, Menardi R (2006) Trephor: a new tool for sampling microcores from tree stems. IAWA Journal 27:89–97.

Rossi S, Deslauriers A, Morin H (2003) Application of the Gompertz equation for the study of xylem cell development. Dendrochronologia 21:33–39.

Schaffhauser A, Curt T, Véla E, Tatoni T (2012) Fire recurrence effects on the abundance of plants grouped by traits in *Quercus suber* L. woodlands and maquis. Forest Ecology and Management 282:157–166.

Schröter D, Cramer W, Leemans R, Prentice IC, Araújo MB, Arnell NW, Bondeau A, Bugmann H, Carter TR, Gracia CA, de la Vega-Leinert AC, Erhard M, Ewert F, Glendining M, House JI, Kankaanpää S, Klein RJT, Lavorel S, Lindner M, Metzger MJ, Meyer J, Mitchell TD, Reginster I, Rounsevell M, Sabaté S, Sitch S, Smith B, Smith J, Smith P, Sykes MT, Thonicke K, Thuiller W, Tuck G, Zaehle S, Zierl B (2005) Ecosystem service supply and vulnerability to global change in Europe. Science 310:1333–1337.

Taneda H, Sperry JS (2008) A case-study of water transport in co-occurring ring- versus diffuse-porous trees: contrasts in water-status, conducting capacity, cavitation and vessel refilling. Tree Physiology 28:1641-1651.

Terwilliger VJ, Kitajima K, Le Roux-Swarthout DJ, Mulkey S, Wright SJ (2001) Intrinsic water-use efficiency and heterotrophic investment in tropical leaf growth of two Neotropical pioneer tree species as estimated from $\delta^{13}C$ values. New Phytologist 152:267–281.

Varner MJ, Putz FE, O'Brien JJ, Kevin Hiers J, Mitchell RJ, Gordon DR (2009) Post-fire tree stress and growth following smoldering duff fires. Forest Ecology and Management 258:2467–2474.

731 Veble D, Brečko Grubar V (2016) Pogostost in obseg požarov v naravi na Krasu in v slovenski
732 Istri / The frequency and extent of wildfires on the Kras and in Slovenian Istria.
733 Geografski vestnik – Geographical Bulletin 88:9–20.
734 Zavod za gozdove Slovenije (2017) Poročilo zavoda za gozdove Slovenije o gozdovih za leto
735 2016 (The Slovenia Forest Service Report on Slovenian forests for 2016). Zavod za
736 gozdove Slovenije, Ljubljana, Slovenia.
737 Zweifel R, Zimmermann L, Zeugin F, Newbery DM (2006) Intra-annual radial growth and water
738 relations of trees: implications towards a growth mechanism. Journal of Experimental
739 Botany 57:1445–1459.

740 **Table captions**

741

742 **Table 1.** Chlorophyll content, net photosynthesis (A), stomatal conductance (g_s), transpiration
743 (E), midday- (Ψ_{midday}) and predawn water potential ($\Psi_{predawn}$) in the leaves of *Quercus pubescens*.
744 Measurements were taken on 21 June (DOY 172), 18 July (DOY 199), 8 August (DOY 220) and
745 24 August (DOY 236). Means ± standard errors are shown, n = 18 for SPAD, A, g_s and E; n = 9
746 for Ψ_{midday} and Ψ_{predaw} for each tree group.

747

	DOY 172	DOY 199	DOY 220	DOY 236
Chlorophyll [SPAD]				
H-trees	37.8 ± 0.58	38.8 ± 0.68	37.6 ± 0.44	39.3 ± 0.35
F-trees	36.6 ± 0.31	37.8 ± 0.41	36.7 ± 0.44	38.2 ± 0.23
A [μmol CO_2 m^{-2} s^{-1}]				
H-trees	3.94 ± 0.36	2.73 ± 0.24	4.49 ± 0.31	3.64 ± 0.29
F-trees	3.02 ± 0.21	10.02 ± 0.56	5.27 ± 0.31	2.60 ± 0.18
g_s [mol H_20 m^{-2} s^{-1}]				
H-trees	0.039 ± 0.003	0.036 ± 0.002	0.051 ± 0.003	0.034 ± 0.002
F-trees	0.053 ± 0.004	0.053 ± 0.003	0.052 ± 0.003	0.048 ± 0.003
E [mmol H_2O m^{-2} s^{-1}]				
H-trees	1.35 ± 0.10	1.36 ± 0.10	1.78 ± 0.10	1.19 ± 0.08
F-trees	1.31 ± 0.08	1.47 ± 0.07	1.70 ± 0.10	1.38 ± 0.08
Ψ_{midday} [MPa]				
H-trees	-2.55 ± 0.05	-2.45 ± 0.03	-1.80 ± 0.05	-3.13 ± 0.02
F-trees	-2.16 ± 0.03	-2.19 ± 0.07	-2.35 ± 0.06	-2.84 ± 0.04
$\Psi_{predawn}$ [MPa]				
H-trees	-	-0.96 ± 0.01	-0.84 ± 0.01	-1.65 ± 0.01
F-trees	-	-0.44 ± 0.01	-0.45 ± 0.01	-0.95 ± 0.02

748

Table 2. Significance of effects, expressed as p-values, of main factors (tree group and day of year-DOY) and their interaction on different leaf parameters. Linear mixed models were used to derive the p-values. Statistically significant effects are bolded. *A*, net photosynthesis; g_s, stomatal conductance; *E*, transpiration; Ψ_{midday}, midday water potential; $\Psi_{predawn}$, predawn water potential.

	ANOVA (p value)		
	Tree group	Doy	Tree group x Doy
Chlorophyll	0.234	**0.016**	0.840
A	**0.007**	0.112	0.082
g_s	0.064	0.450	0.356
E	0.770	0.275	0.359
Ψ_{midday}	**<0.001**	**<0.001**	**0.003**
$\Psi_{predawn}$	0.580	**<0.001**	**0.006**

Table 3. Main wood and phloem formation milestones in *Quercus pubescens* in 2017 (*n* = 6 for F-trees and H-trees). Significant effects at 0.05 significance level are in bold. F-trees, fire-damaged trees; H-trees, undamaged trees.

	Day of the year ± standard deviation		
Variable	F-trees	H-trees	*F* value (p value)
Transition from early phloem to late phloem	148.5 ± 9.8	153.2 ± 8.7	0.758 (0.404)
Transition from earlywood to latewood	147.8 ± 5.8	150.0 ± 3.3	0.636 (0.446)
Completely formed earlywood	171.7 ± 3.3	166.0 ± 5.9	4.275 (0.0655)
End of cell production	212.0 ± 17.0	192.0 ± 2.4	**8.152 (0.0171)**
End of xylem formation	288.0 ± 7.7	288.0 ± 7.7	0 (1)
Appearance of tyloses in xylem increment of 2016	94.7 ± 6.7	120.0 ± 9.1	**30.11 (0.0003)**
Appearance of tyloses in xylem increment of 2017	221.3 ± 20.8	242.3 ± 20.8	**5.075 (0.0479)**

Table 4. ANOVA results of the contribution of main effects (tree group, tree part and year) to the xylem and phloem anatomical features during the 2017 growing season (n = 6 for F-trees and H-trees). Significant effects at 0.05 significance level are bolded.

Variable	Tree group *F* value (p value)	Tree part *F* value (p value)	Year *F* value (p value)
Xylem-ring width	**46.958 (0.000)**	**24.610 (0.000)**	**5.820 (0.005)**
Earlywood width	**28.062 (0.000)**	**36.323 (0.000)**	**5.396 (0.006)**
Latewood width	**162.838 (0.000)**	**52.436 (0.000)**	**18.024 (0.000)**
Mean initial earlywood vessel size	1.445 (0.230)	**64.766 (0.000)**	0.282 (0.754)
Mean initial earlywood vessel area	**4.137 (0.043)**	**126.210 (0.000)**	0.511 (0.601)
Mean earlywood vessel size	2.842 (0.093)	**52.249 (0.000)**	0.808 (0.446)
Mean earlywood vessel area	3.831 (0.051)	**81.119 (0.000)**	1.145 (0.319)
Vessel density	2.598 (0.111)	**29.342 (0.000)**	**3.430 (0.038)**
Phloem-ring width	**4.830 (0.039)**	**9.514 (0.001)**	/
Early phloem width	0.079 (0.781)	**9.696 (0.001**)	/
Late phloem width	**27.938 (0.000)**	**12.630 (0.000)**	/
Mean sieve tube size	**20.062 (0.000)**	**43.706 (0.000)**	/
Mean sieve tube area	**25.704 (0.000)**	**100.954 (0.000)**	/

Figure captions

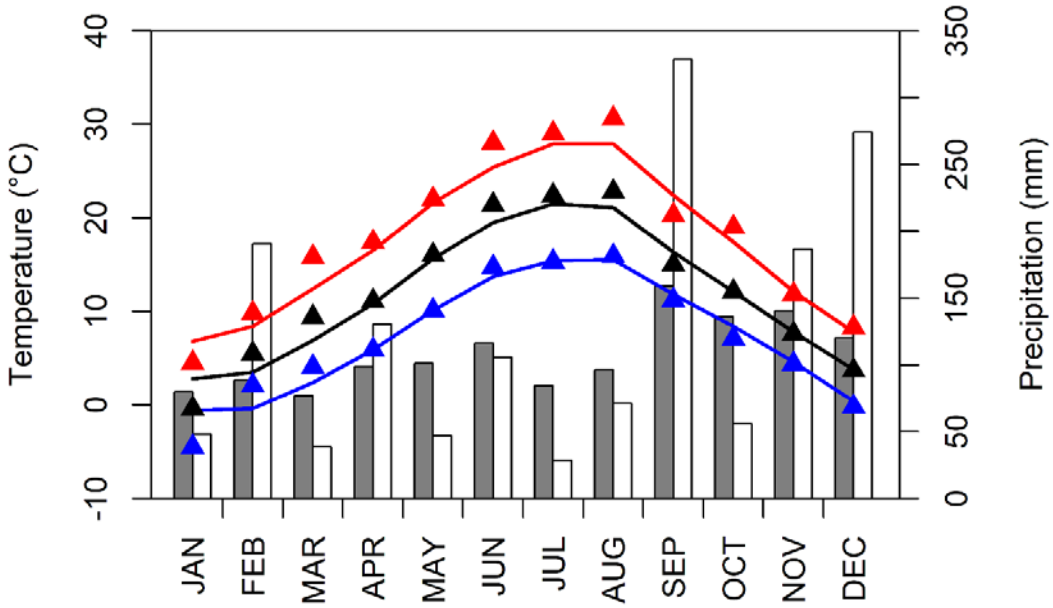

Figure 1. Mean climatic conditions for the period 1992–2017 and conditions in 2017 on the Podgorski Kras experimental site. Mean monthly temperatures: mean (black line), minimum (blue line) and maximum (red line), and amount of monthly precipitation (grey columns), averaged for the period 1992–2017. Mean monthly temperatures: mean (black triangles), minimum (blue triangles) and maximum (red triangles), and amount of monthly precipitation (white columns) in 2017.

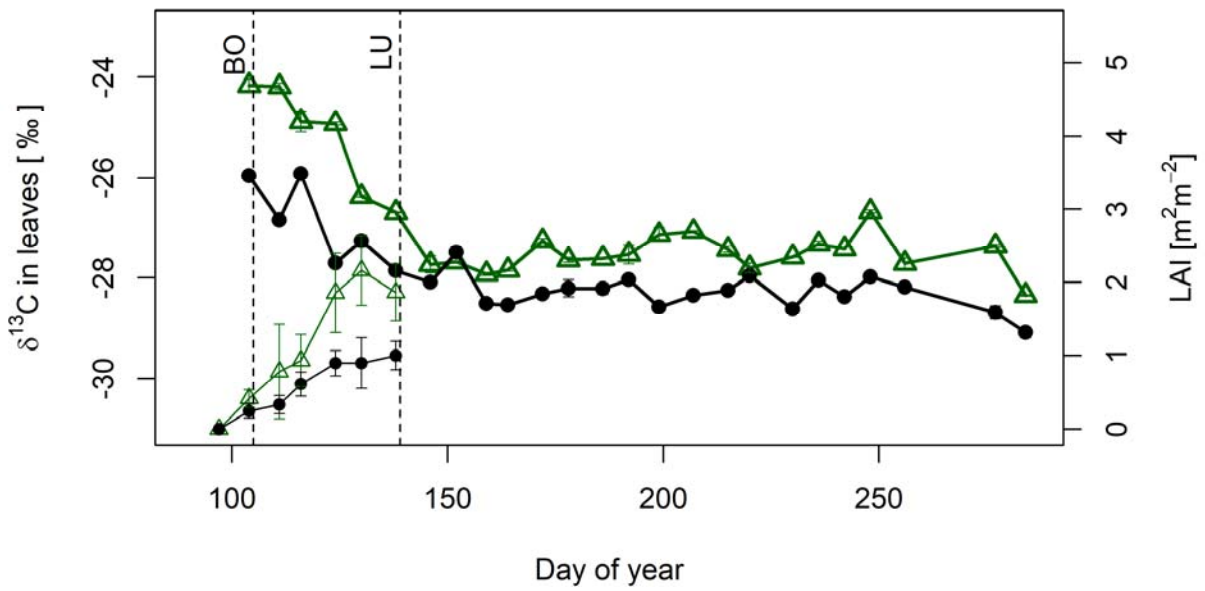

774

775 **Figure 2.** Seasonal variation in carbon isotope composition ($\delta^{13}C$; bold solid lines) in leaves and
776 LAI (thin solid lines) in leaves of H-trees (green) and F-trees (black) of *Quercus pubescens* in
777 2017 (n = 6 for H and F-trees, pooled samples). Points represent means ± standard error. BO, bud
778 opening; LU, full leaf unfolding.

779

780

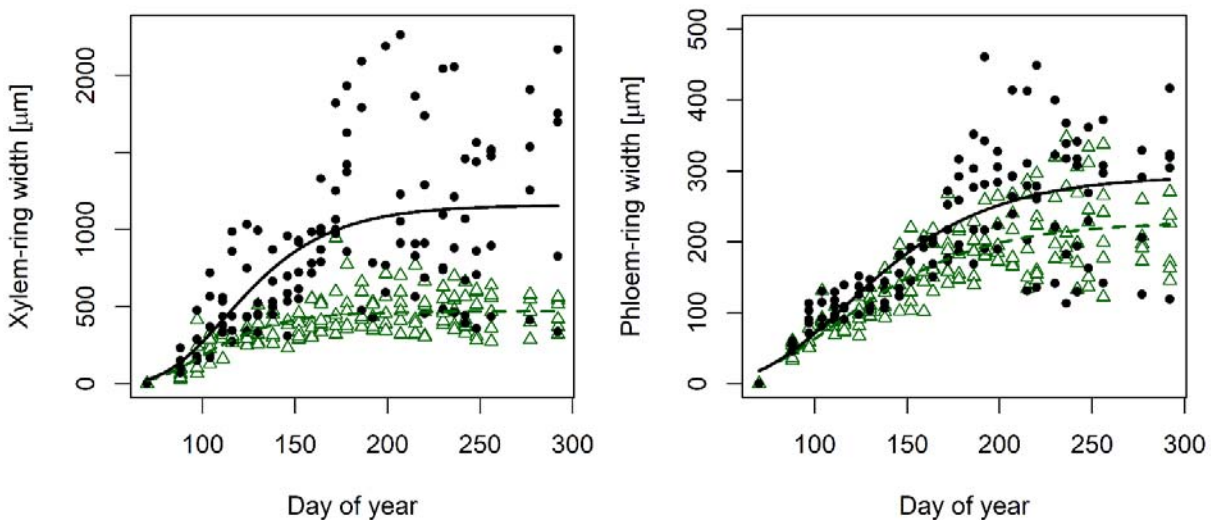

781

782 **Figure 3.** Xylem and phloem formation dynamics in H-trees (green) and F-trees (black) of
783 *Quercus pubescens* in 2017. Green triangles (H-trees, *n*= 6) and black dots (F-trees, *n* = 6)
784 represent individual measurements, while green dashed (H-trees) and black solid (F-trees) lines
785 represent fitted Gompertz functions.

786

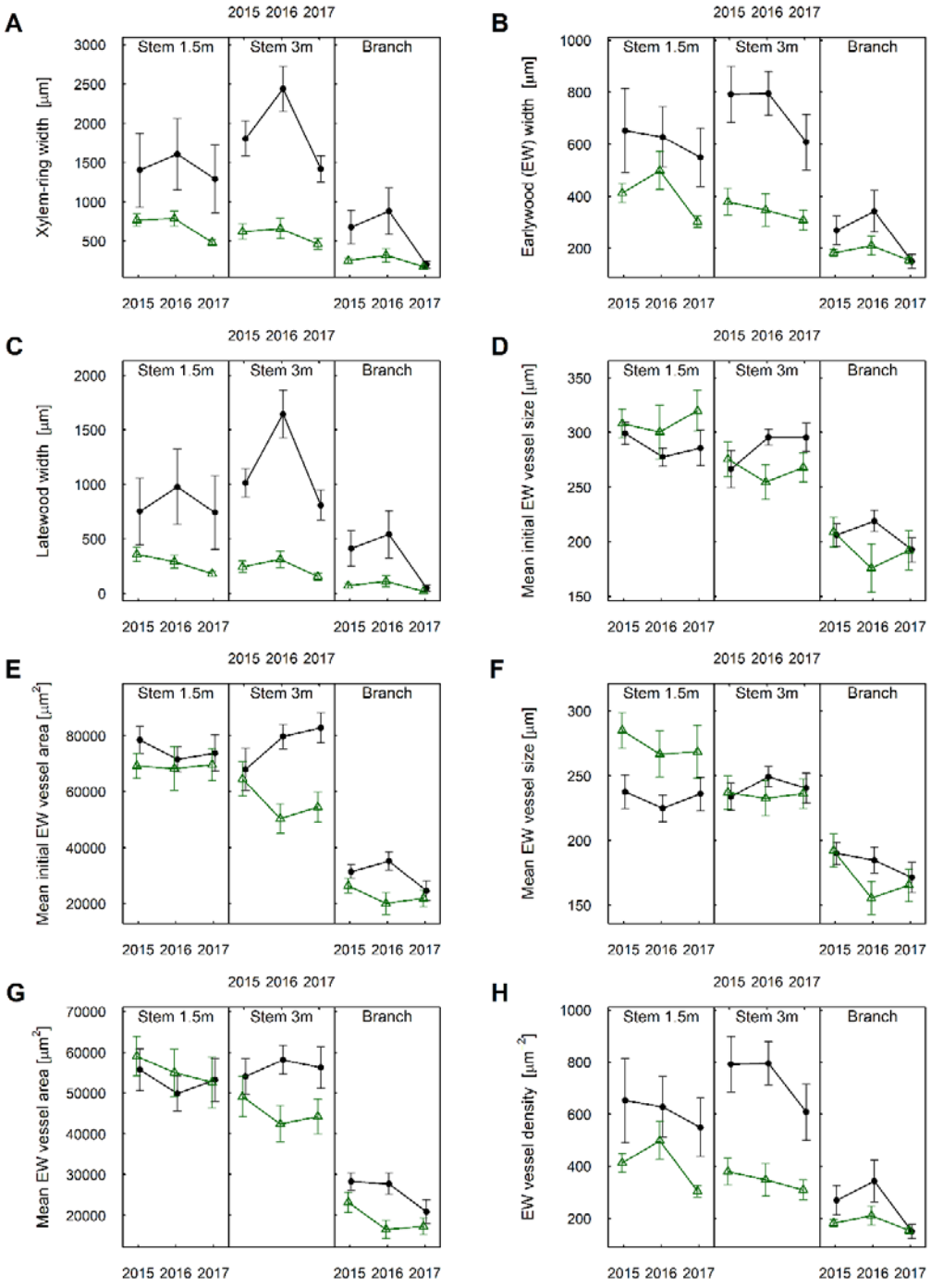

787

788 **Figure 4.** Xylem anatomy parameters in years 2015–2017 for fire damaged (black) and

789 undamaged trees (green) in different woody parts of the tree. D1.5, sampling at stem 1.5 m above

790 the ground; D3, sampling at stem 3 m above the ground; V3, sampling at branch 3 m from the

791 apex.

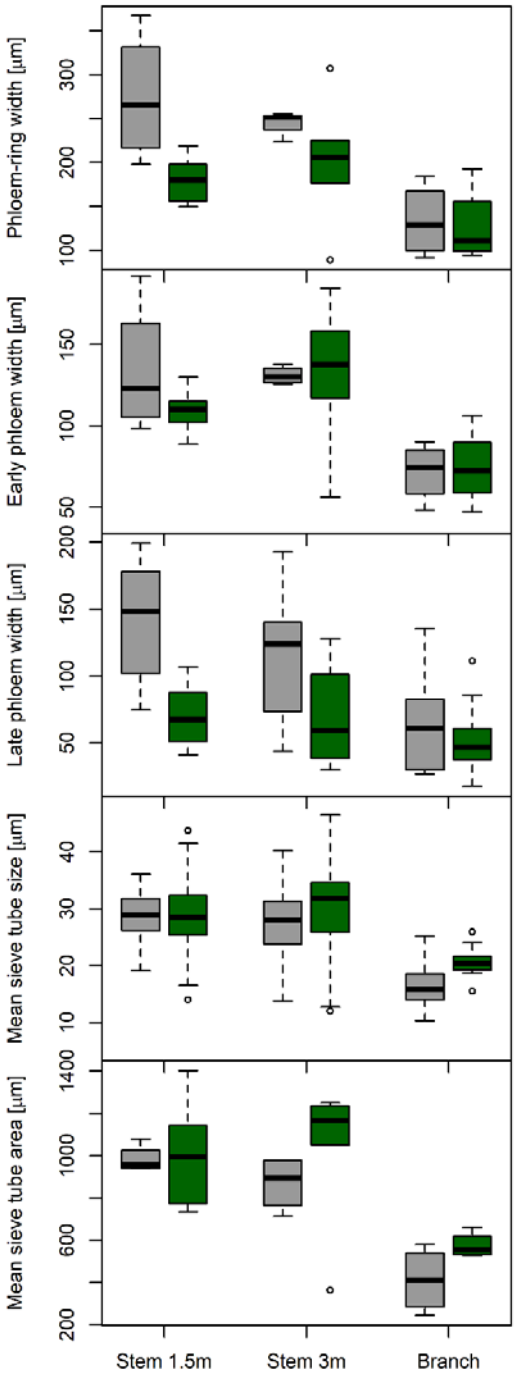

792

793 **Figure 5.** Phloem anatomy parameters in 2017 for fire damaged (grey) and undamaged trees
794 (green) in different parts of the tree: in stem at 1.5 above the ground, in stem at 3 m above the
795 ground and in branch 3 m from the apex. Sieve tubes of early phloem were measured.